Characteristics of ship generated wave field in sub, transient and super critical regions

Mohamed A. Kotb
Marine and Naval Architecture Dept. Faculty of Eng., Alexandria University, Alexandria, Egypt
Kotb2000@yahoo.com

Ships moving in still water disturb the water surface and generate a system of waves. The generated waves may be of sufficient magnitude to disturb the surrounding environment causing harmful effects. The wash from ships particularly at high speeds can cause damage and may endanger life. If the energy contained is dispersed in shallow water near a beach or a river bank, the bank may be eroded away. In recent years, wash has received more attention than usual particularly with the increase in the service speed required of certain vessels. The ship generated waves have become an issue of international importance, especially for densely populated and active harbor areas. Therefore, a knowledge of the characteristics of the waves generated is required in order to quantify and reduce their possible harmful effects. This knowledge also can greatly assist in establishing allowable vessel speeds in navigable waterways, monitoring of riverbank erosion; design of bank erosion control structures, design of marina protective works; minimize motions of moored floating objects, and develop prediction techniques. The purpose of this work is to discuss the major factors influencing wave wake characteristics in deep and shallow waters. It is well known that the waves generated in shallow water are different than those generated in deep water. A computational study was carried out on a simple 2D floating strut over a range of operating conditions and the wave pattern parameters variations were quantified and commented upon.

عندما تتحرك السفينة في المياه ينشأ عنها امواج وتلك الأمواج تحتوي علي قدر كبير من الطاقة ولاسيما تلك الأمواج الناشئة عن حركة السفن السريعة الأمر الذي قد يتسبب في حدوث بعض الأضرار للبيئة المحيطة من شواطئ وضفاف الأنهر والبحيرات والنباتات البحرية وايضا الأرصفة والسفن االمتراكية اذا ما وصلتها تلك الأمواج. و من ثم فان المعرفة الجيدة لطبيعة تلك الأمواج وخصائصها من شانه أن يساعد في تجنب الأضرار التي قد تنشأ عنها كما يساعد في وضع حد أعلي وامن لسرعات السفن واليخوت وفي تصميم وسائل حماية الشواطئ والسفن المتراكية وكوسيلة لتوثيق خصائص تلك الأمواج فان البحث الحالي يتناول طريقة حساب تلك الأمواج المتولدة عن حركة السفن في كل من المياه العميقة والضحلة.

Keywords: Ship generated waves, Depth Froude number, Ship wash, Shallow waters, Environmental effects

1. Introduction

A ship moving in still water induces a varying pressure field above and below the free stream pressure. This pressure field disturbs the water surface and results in elevations and depressions around and past the hull. These water disturbances are known as ship generated waves.

These waves propagate out from the vessel, particularly from the bow and the stern with different heights, periods, and lengths depending on the distribution of the pressure field around the hull which in turn depends upon the ship speed, hull form, draft, trim, and water depth.

A number of problems are associated with ship-generated waves. Examples include bank erosion, nuisance to other users, damage to jetties and/or river walls, safety risk to small vessels, destruction of fragile water plants, motions of moored objects and damage to the ecology of intertidal and shallow sub-tidal habitat. Several studies confirmed the undesirable impacts of ship wake wash, e.g. Johnson [1].

Therefore, a knowledge of the characteristics of the ship generated waves is required in order to quantify and reduce their possible harmful effects.

This knowledge also can greatly assist in setting allowable vessel speeds in navigable

waterways, monitoring of riverbank erosion; design of marina protective and control structures; minimizing motions of moored floating objects, and developing prediction techniques.

Research in the literature has provided such knowledge, e.g. Sorensen and Weggel [2]. Most of the data reported are related to certain ships or specific navigational waterways, and as such the results can not be generalized or attributed to specific parameters in clearly defined way.

The purpose of this work is to discuss the major factors influencing wave wake characteristics, throw some light on parameters describing wave field and their functional dependence on operating conditions in deep and shallow waters. This is thought to be better illustrated through simple shapes.

2. Ship generated wave regions

Wave pattern depends on a number of factors. These factors can be grouped in two non dimensional parameters. These are length Froude's number, and depth Froude's number which are defined as:

$$F_{nL} = \frac{V}{\sqrt{gL}}. \quad (1)$$

$$F_{nh} = \frac{V}{\sqrt{gh}}, \quad (2)$$

where L is ship length and h is water depth. Fig. 1 shows the scale by which operation regimes are defined.

Length Froude number is used for ships operating in deep water, while depth Froude number is more applicable to shallow water operation. The 0.4 length Froude number value is considered critical on this scale where transverse wavelength equals ship's length.
On the otherhand, the value of 1.0 is marked critical on the depth Froude number scale. The reasons will be explained in the following paragraphs.

Critical depth Froude number value of 1.0 is analogous to Mach one value in aerodynamics. Maximum wave speed at a particular water depth is used to normalize ship speed in a way similar to normalizing aircraft speed using the speed of sound.

2.1. Wave propagation

The speed of the surface wave c is given in terms of water depth h and wave length λ by:

$$c = \sqrt{\frac{g\lambda}{2\pi}\tanh\left(\frac{2\pi h}{\lambda}\right)}, \quad (3)$$

and the corresponding wave period T_P is given by

$$T_P = \frac{\lambda}{c} = \sqrt{\frac{2\pi\lambda}{g}\operatorname{cotanh}\left(\frac{2\pi h}{\lambda}\right)}. \quad (4)$$

Figs. 2 and 3 display contours of c and T_P on a grid of wave length λ and water depth h. From these figures, we note that when the water depth is less than approximately half the length of the wave the wave celerity is only a function of wave length while when this ratio is less than 0.05 the celerity is function of water depth only. This observation leads to the distinction of three flow regimes; namely deep, transitionally shallow, and shallow water regions. Table 1 shows the applicable relations for the three regions.

3. Ship generated wave pattern parameters

3.1. Infinite water depth

The wave pattern generated by a moving point at low speeds or relatively large water depth (Fn_h=0) consists of symmetrical pairs of diverging waves that move obliquely out from the vessel sailing line and a single set of transverse waves that move forward in the direction of the sailing line.

The transverse and diverging waves meet to form cusps which are located along lines that are $19^0\,28'$ out from the sailing line. The largest wave amplitudes are at the cusps. This is known as Kelvin pattern [3].

According to Kelvin the wave pattern due to single pressure point moving at speed V as shown on fig. 4 is given by the parametric equations:

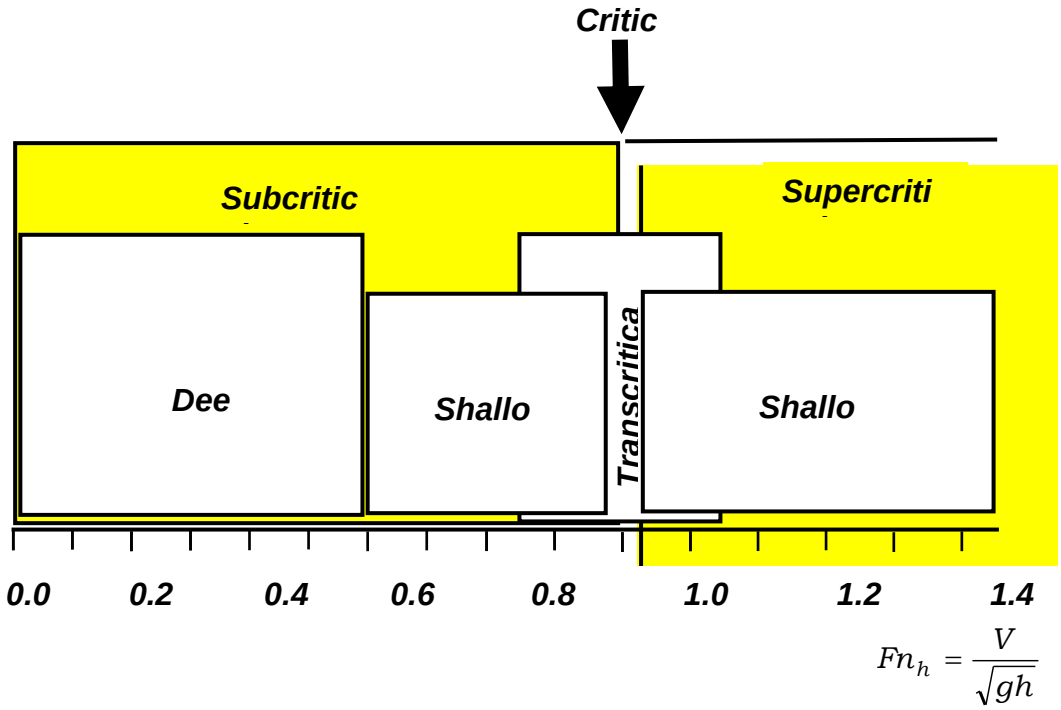

Fig.1. Depth Froude number scale.

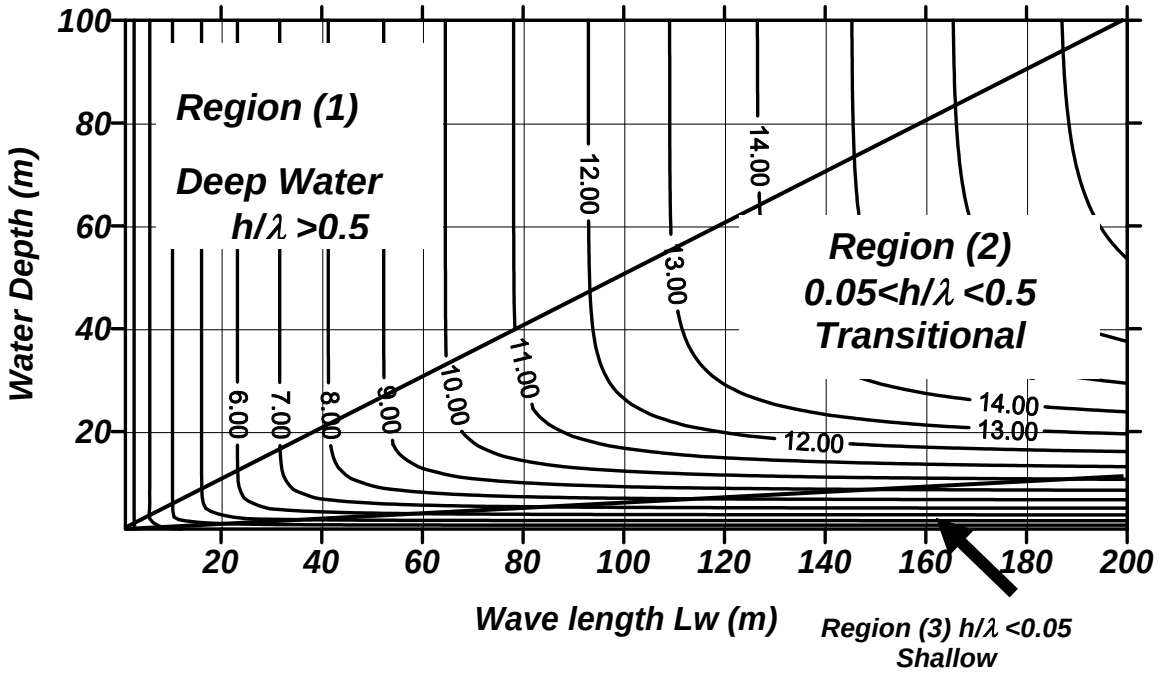

Fig. 2. Wave celerity contours.

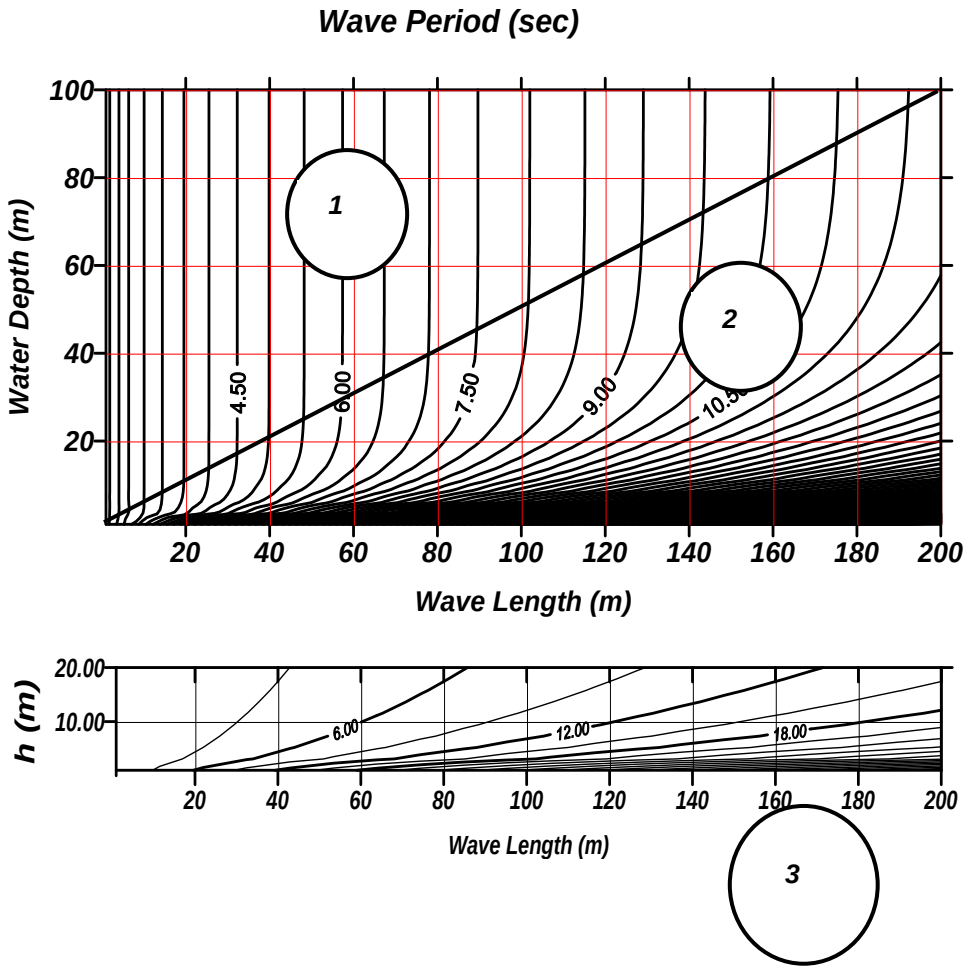

Fig. 3. Wave period contours.

Table 1
Applicable wave formulae for different depth regions

Condition	Wave celerity	Wave period	Remarks
$\frac{h}{\lambda} \geq 0.5$	$c = \sqrt{\frac{g\lambda}{2\pi}} \approx 1.25\sqrt{\lambda}$	$T_p = \sqrt{\frac{2\pi\lambda}{g}} \approx 0.80\sqrt{\lambda}$	deep water
$0.5 \geq \frac{h}{\lambda} \geq 0.05$	$c = \sqrt{\frac{g\lambda}{2\pi}\tanh\left(\frac{2\pi h}{\lambda}\right)}$	$T_P = \frac{\lambda}{c} = \sqrt{\frac{2\pi\lambda}{g}\cot anh\left(\frac{2\pi h}{\lambda}\right)}$	transitionally shallow
$\frac{h}{\lambda} \leq 0.05$	$c = \sqrt{gh}$	$T_p = \frac{\lambda}{\sqrt{gh}} \approx 0.319\frac{\lambda}{\sqrt{h}}$	shallow water

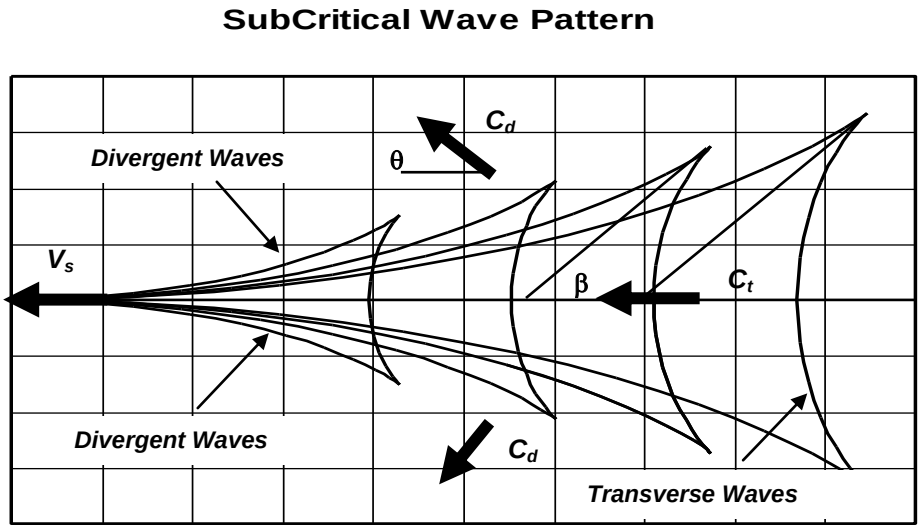

Fig. 4. Wave pattern in deep water (single pressure point).

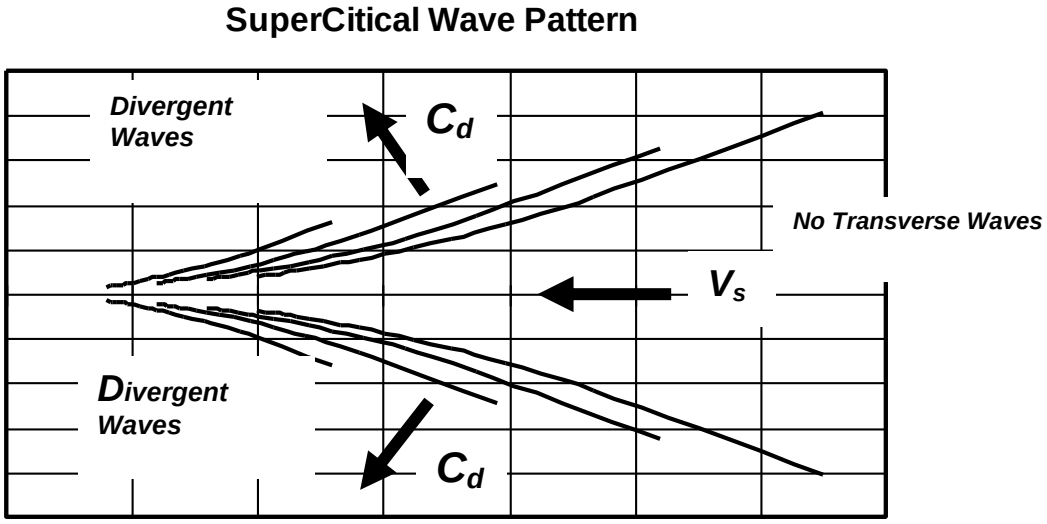

Fig. 5. Wave pattern in super critical region.

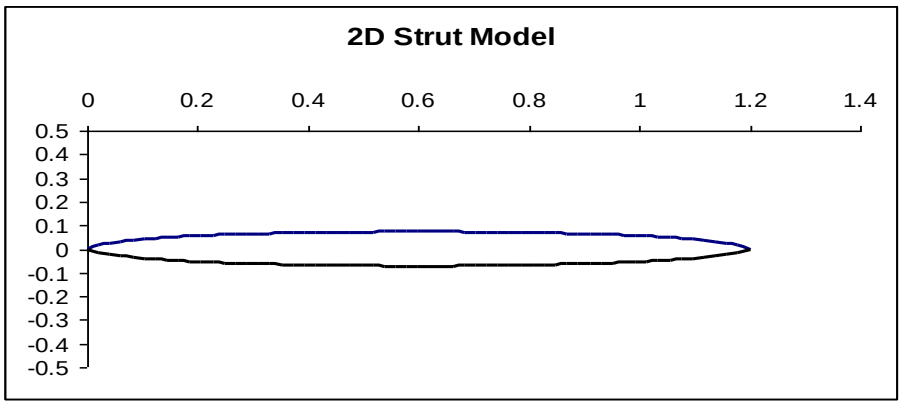

Fig. 6. Case study cross section strut.

$$x = \frac{V^2\psi}{g}\cos\beta\left(1+\sin^2\beta\right), \tag{5}$$

$$y = -\frac{V^2\psi}{g}\cos^2\beta\sin\beta\,. \tag{6}$$

If the vessel speed is increased, the wave lengths would accordingly increase, but the overall pattern (including the $19^0 28'$ angle) would retain the same form. For diverging waves in deep water (Fn_h =0) the theoretical propagation angle is 35° 16' and the diverging wave crests oblique angle at the cusp is 54° 44'.

As shown in fig. 4, the celerity of the transverse waves C_t is equal to the speed of the ship Vs, whereas the celerity of the diverging waves C_d is equal to the ship speed projected onto the propagation direction of the diverging waves. That is, in deep water:

$$C_t = V\,. \tag{7}$$

$$C_d = V\cos\theta\,. \tag{8}$$

From the above expressions, the wave period for transverse and diverging waves in deep water are

$$(T_P)_t = \frac{2\pi V}{g}\,. \tag{9}$$

$$(T_P)_d = \frac{2\pi V\cos\theta_d}{g}\,. \tag{10}$$

The deep water pattern (Kelvin waves) remains almost unchanged for depth Froude' number up to 0.6-0.7.

3.2. Finite water depth (depth-Froude number > 0.6-0.7)

As the vessel speed increases causing the generated wave lengths to increase, the waves may become long enough to "feel" the seabed (h/λ < 0.5). This occurs when the depth Froude number exceeds approximately 0.7 and wave pattern will be different from the deep water wave pattern.

As the Froude number increases from 0.7 to 1.0, the transverse wave heights increase faster than the diverging wave heights, becoming more prominent towards F_{nh} = 1. Concurrently, the cusp locus angle increases from 19^0 18' to 90° at Fn_h = 1. At Fn_h = 1, with the cusp locus angle equal to 90°, the diverging and transverse waves have coalesced with their crests oriented perpendicular to the sailing line. Also, most of the energy in the wave system is concentrated in the first wave at the bow.

Havelock, as reported in [3] extended the solution of the problem of wave formation behind a pressure impulse to the case of finite depth of a fluid h. The wave system is contained with an angle 2α given by the equation:

$$\alpha = \cos^{-1}\left[\frac{\sqrt{8(1-n)}}{(3-n)}\right]. \tag{11}$$

The value of n is given by:

$$n = \frac{4\pi(h/\lambda)}{\sinh(4\pi(h/\lambda))}, \tag{12}$$

n=0 when $h=\infty$ and n=1 when $V=\sqrt{gh}$

The h/λ value is obtained if the value of Fn_h is known from the relation:

$$F_{nh} = \sqrt{\frac{(h/\lambda)}{2\pi}\tanh(2\pi(h/\lambda))}\,. \tag{13}$$

As it was mentioned earlier, the divergent wave propagation angle in deep water is 35.276^0. This value remains almost constant for Fn_h up to 0.6-0.7. As a consequence of Kelvin cone angle increase after 0.6 Fn_h the propagation angle decreases till zero at Fn_h =1.0.

Weggel and Sorensen [2] proposed the following empirical expression for the wave propagation direction of the diverging waves as a function of Fn_h for depth Froude numbers less than 1:

$$\theta = 35.267^\circ\left[1-\exp(12(Fnh-1))\right] \quad Fnh<1\,. \tag{14}$$

3.3. Finite water depth (Fn_h > 1.0)

For Froude numbers in excess of unity, since the greatest wave celerity can only equal $\sqrt{gh}$, no transverse waves can exist. Diverging waves extend back from the vessel and form an angle equal to

$$\beta = \sin^{-1}\left(\frac{1}{F_{nh}}\right), \tag{15}$$

with the sailing line. This situation is similar to the Mach angle in compressible flows where:

$$\mu = \sin^{-1}\left(\frac{1}{M}\right). \tag{16}$$

Yih and Zhu [4] derived a mathematical model, for predicting the wave patterns created by a moving disturbance. Formulae for the phase lines are given in terms of depth Froude number in parametric eqs. (17 and 18) in the sailing direction x and lateral direction y as:

$$x = -\frac{2\pi n h\phi'\sqrt{\left(k^2-\phi^2\right)}}{k\left(\phi - k\phi'\right)}, \tag{17}$$

$$y = -\frac{2\pi n h\left(k - \phi\phi'\right)}{k\left(\phi - k\phi'\right)}, \tag{18}$$

where

$$\phi = \frac{\sqrt{k\tanh k}}{F_{nh}^2}\ . \tag{19}$$

$$\phi' = \frac{\partial\phi}{\partial k}, \tag{20}$$

k is the wave number, ϕ' is derivative of ϕ with respect to k and n = 1,2,3... indicates a crest and n = 1/2,3/2,5/2... indicates a trough. Eqs. (14-17) are used to produce the wave pattern shown in fig. 5 for supercritical regions.

For a depth Froude number larger than 1, the transverse waves disappear and the diverging waves remain. The wave propagation direction increases for increasing depth Froude numbers, ie the angle between the wave fronts and the navigation track decreases.

4. Ship generated waves calculations

Ship waves have been systematically studied by many authors. Earliest researchers include Froude, Kelvin, Havelock, Mitchell, and Wigley. Summaries of these development can be found in Lamb [5], and Stoker [6]. Raven [7] developed analytical methods for ship wave problem.

The thin-ship theory is based on the mathematical derivations of Mitchell. The theory has been further refined into sophisticated analysis tools by Tuck et al. [8]. In this work, the thin-ship theory was applied to compute ship generated wave patterns.

4.1. Governing equations

The Michell boundary-value problem is given by Laplace's equation

$$\frac{\partial^2\phi}{\partial x^2} + \frac{\partial^2\phi}{\partial y^2} + \frac{\partial^2\phi}{\partial z^2} = 0 \qquad \text{in } -h < z < 0, \tag{21}$$

with the following boundary conditions

The bottom condition at z=−h:

$$\frac{\partial\phi}{\partial x} = 0 \qquad on \quad z = -h\ . \tag{22}$$

The free-surface condition:

$$\frac{g}{U^2}\frac{\partial\phi}{\partial x} + \frac{\partial^2\phi}{\partial x^2} = 0 \qquad on \qquad z = 0\ . \tag{23}$$

The linearised (Michell) hull boundary condition:

$$\frac{\partial\phi}{\partial y} = \pm V\frac{\partial Y(x,z)}{\partial x} \quad on \qquad y = 0\ , \tag{24}$$

where the hull is assumed to be laterally symmetric and the surface is given by $y = Y(x,z)$

The thin-ship theory of Michell represents the body by a centreplane source distribution proportional to its longitudinal rate of change of thickness (local beam). The only requirement for its validity is that the quantity be small. Hence the theory applies to submerged as well as surface-piercing bodies.

4.2. Free surface elevations

The steady surface wave pattern $z = z(x,y)$ of any moving body, as seen at a point (*x, y*) sufficiently far from the ship, is of the form of a sum of plane waves traveling at various angles θ of propagation relative to the direction of motion of the body. Thus:

$$z(x,y) = \mathrm{Re}\int_{-\pi/2}^{\pi/2} A(\theta) e^{-ik[x\cos(\theta)+y\sin(\theta)]} d\theta\,, \qquad (25)$$

where $A(\theta)$ is the free wave spectrum, $k = k_0 \sec^2\theta \tanh(kh)$ and $k_o = \dfrac{g}{V^2}$.

Once $A(\theta)$ is specified, eq. (25) can be used to determine the actual wave pattern. At any given speed *V*, the amplitude function $A(\theta)$ is a property only of the body's hull geometry.

The free wave spectrum $A(\theta)$ for water depth h is given by:

$$A(\theta) = -\frac{2i}{\pi}\frac{k^2}{1-k_0 h\sec^2\theta\sec h^2 kh} \left[\iint Y(x,z)\frac{\cosh k(z+h)}{\cosh kh} e^{ikx\cos\theta} dxdz\right]. \qquad (26)$$

The above holds for all θ in the subcritical range $k_0h > 1$. In the supercritical range $k_0h < 1$, the spectrum *A* is identically zero for all abs(θ) < θ_0 where cos $\theta_o = k_0h$.

We can deduce the wave spectrum $A(\theta)$ in infinite water depth by taking the limit of eq. (26) when h tends to infinity:

$$A(\theta)\big|_{\inf inie} = \lim_{h\to\infty}\frac{2}{\pi}\frac{k}{1-k_0 h\sec^2\theta\sec h^2 kh} \iint Y_x(x,z)\frac{\cosh k(z+h)}{\cosh kh} e^{ikx\cos\theta} dxdz\,. \qquad (27)$$

At the limit when *h* is very large we get:

$$k \to k_o \sec^2(\theta)\,. \qquad (28)$$

$$1 - k_0 h\sec^2\theta\sec h^2 kh \to 1\,, \qquad (29)$$

$$\frac{\cosh k(z+h)}{\cosh kh} \to e^{-kz}\,. \qquad (30)$$

Substituting the limits given by eqs. (28-29 and eq. (30) in eq. (27) we get:

$$A(\theta)\big|_{\inf inie} = .-\frac{2i}{\pi}k^2\left[\iint Y(x,z)e^{-kz}e^{ikx\cos\theta}dxdz\right] \qquad (31)$$

The double integral in either eqs. (26 or 31) over the body's centreplane, determines $A(\theta)$ for each fixed angle θ from the offsets *Y*(*x,z*), and can be reduced to a pair of separate integrals over depth and length. Details can be found in eqs. (9 and 10). Expressions for $A(\theta)$ are used together with eq. (25) to solve for wave elevations. A number of routines exist for conducting such calculations, e.g. Mitchlet code eq. (11).

5. Case study

The procedure explained above was applied to a simple 2D body "strut like" to calculate the wave pattern generated due to its motion. The results were analyzed and the characterizing parameters were deduced. The 2D model data geometrical particulars are given in fig. 6.

The model was examined at a range of depth Froude number (0 to 1.5) at a fixed length Froude number of 0.35. Table 2 summarizes the operating conditions.

6. Results

Figs. 7-a and 7-b show contours and surface presentation of ship model generated waves in deep water moving at 1.184 m/s speed. The main wave system components such as wave length, oblique angle, propagation angle and finally the envelope angle are depicted on the surface plot, 7-b. The data domain shown has a length of 7L and a width of 5L where L is the model length.

A number of several transverse waves approximately normal to the direction of motion, past the model are shown. These waves represent combined bow and stern transverse system. This number is directly related to model speed for the speed of 1.184 m/s the transverse waves length is 0.898 m which is 0.74 L. Divergent waves originating from the model are clearly shown.

Both transverse and divergent waves from the model is contained within a wedge with half angle 19 degrees to the direction of motion of the ship. Divergent waves are obliqued to the sailing line at about 55 degrees. These waves propagate away from the ship track at about 35 degrees. For the rectangular region studied maximum and minimum amplitudes are in the range of +-0.012 m.

The deep water case was thoroughly examined and the characterizing parameters evaluated. This was a necessary step in assessing and comparing the wave pattern when moving to differential flow regions either by moving at higher speed or operating in finite water depth.

Further computation results indicated that the wave pattern resembling sailing in deep water remains unchanged for depth Froude number values up to 0.6. Fig. 8 shows wave pattern generated at 0.5 depth Froude number which is not much different from results at lower Froude numbers.

Further reduction in water depth (e.g. Fn_h= 0.8) produces different wave pattern as depicted in fig. 9. One can conclude that the generated waves started to feel the ground proximity. This is reflected on slight widening of the enveloping wedge and increased wave length and periods, in addition to different wave directions, …etc.

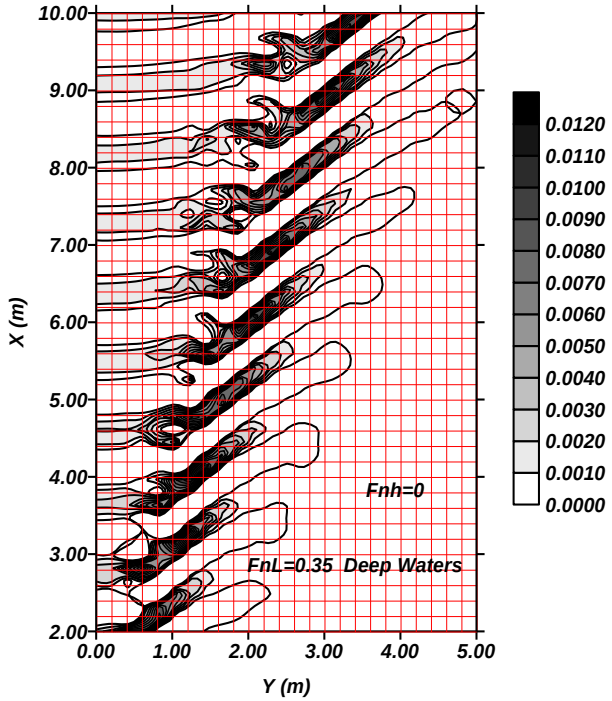

Fig. 7-a. Wave contours fo the case study at Fn_h = 0 and Fn_L = 0.35.

Table 2
Operating conditions for the case study

Fnh	Condition	Remarks	Depth (m)
0		Infinite	Infinite
0.3		"Deep"	1.58
0.5	Subcritical		0.571
0.6			0.397
0.7		Shallow	0.291
0.8			0.223
0.9	Transcritical		0.1764
1	Critical		0. 1429
1.1	Transcritical		0.1181
1.5	Supercritical		0.0635

Results at Fnh=1.1 indicate the disappearance of transverse waves, see fig. 10. This feature continues to prevail at higher Froude number as shown in fig. 11 for the case of 1.5 F_{nh}. As the depth-based Froude number is increased further, the angle of the enveloping wedge continues to decrease, and the wave pattern contains only diverging waves.

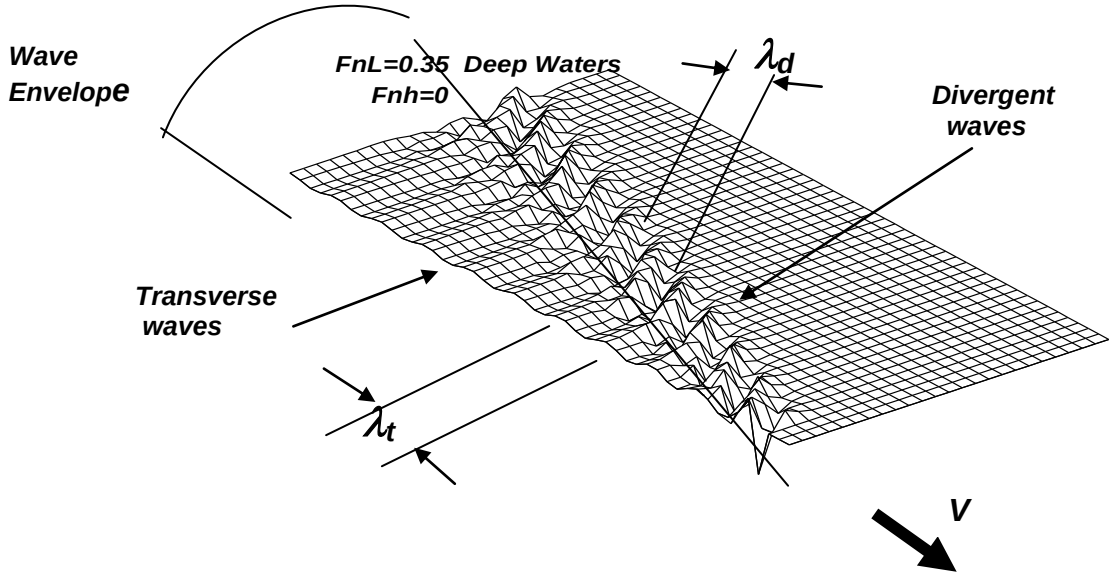

Fig. 7-b. Wave surface elevations for the case study at Fnh=0 and FnL=0.35.

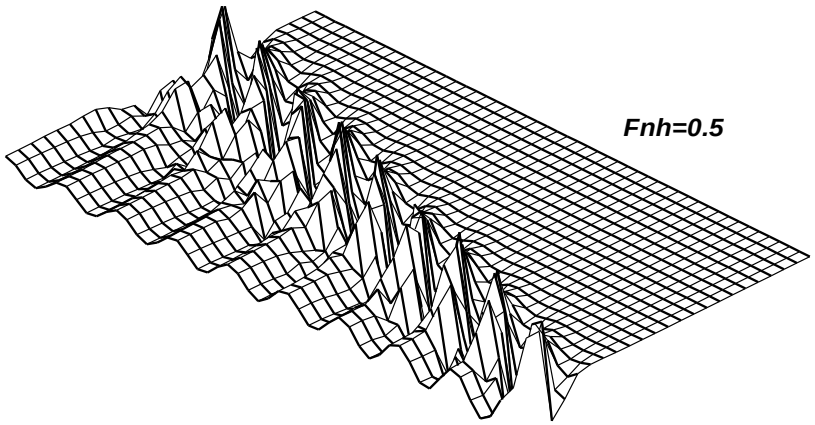

Fig. 8. Wave surface elevations for the case study at Fnh=0.5 and FnL=0.35.

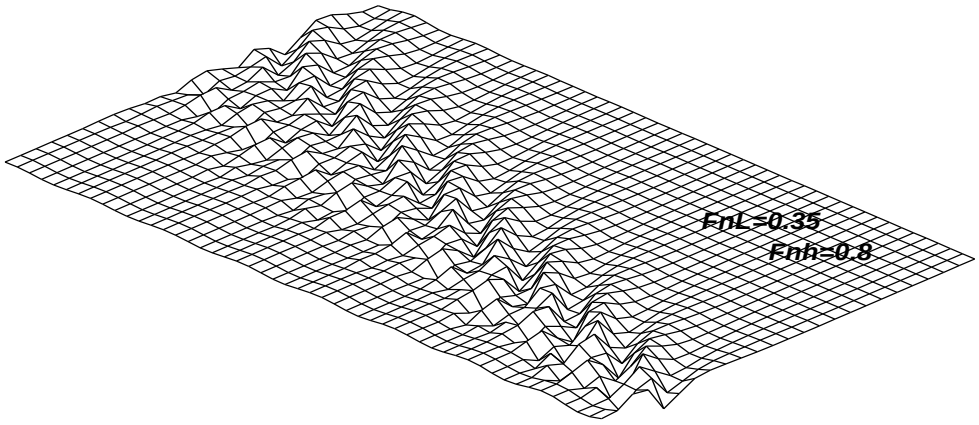

Fig. 9. Wave surface elevations for the case study at Fnh=0.8 and FnL=0.35.

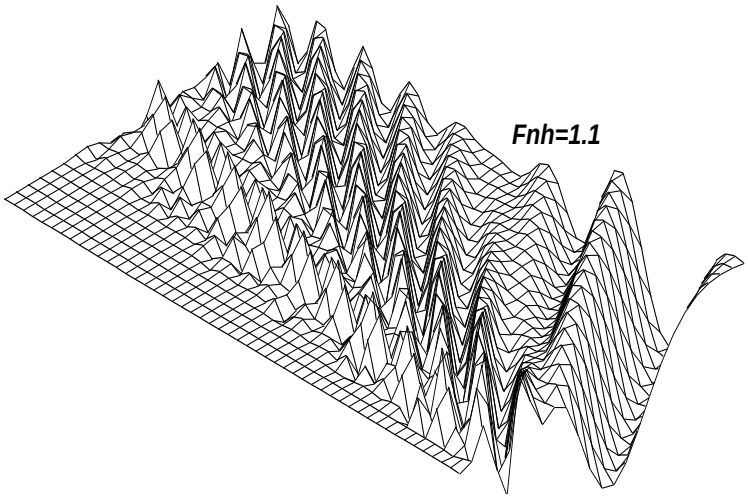

Fig. 10. Wave surface elevations for the case study at Fnh=1.1 and FnL=0.35.

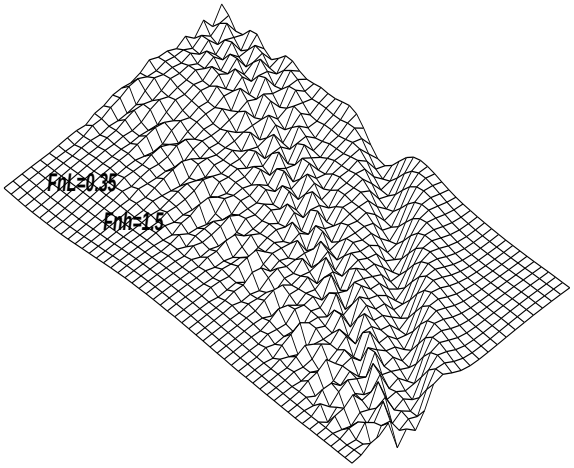

Fig. 11. Wave surface elevations for the case study at Fnh=1.5 and FnL=0.35. Logitudinal.

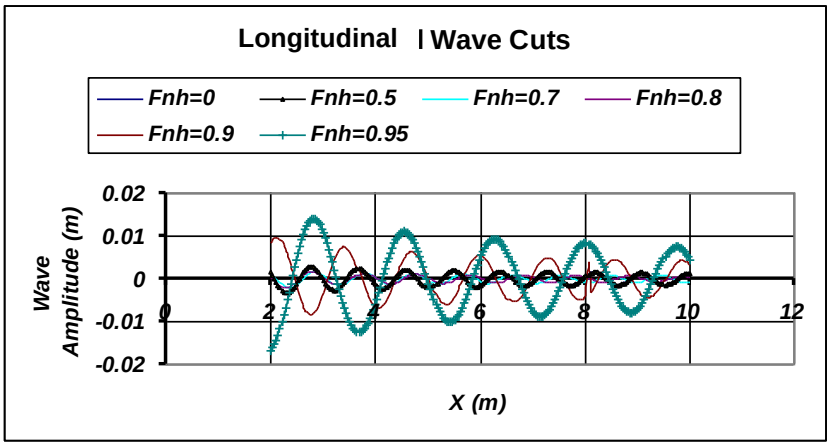

Fig. 12. Logitudinal wave cuts (case study) at different depth froude numbers at Fn_L = 0.35.

Longitudinal wave cuts along the sailing line display wave height variations for the transverse waves. These heights decay in the downstream direction, fig. 12.

A number of transverse wave cuts were taken at 2.5 m downstream at different depth Froude numbers as shown in fig. 13. The transverse cuts have the advantages of illustrating both transverse (around the center) and divergent wave systems (peaks at the profile edges). Distance between the two peaks get larger as one goes downstream.

The computed wave data was compiled to quantify the ship generated wave system parameters. One of these parameters is the envelope angle which contains the wave system. To assess this parameter in conditions other than deep water, the wave crest amplitudes envelope at different radial cuts at different angles are calculated and plotted for constant value of depth Froude number. Sample of such plots are given in fig. 14. From such curves it was clear that there exist an angle at which the wave heights are maximum. This condition defines the line of cusps where transverse and divergent waves meet. Fig. 15 shows the line of cusps angle variation with depth Froude number where almost negligible variation up to 0.7 F_{nh} after which slight increase is exhibited up to 0.95 F_{nh} where it peaks up to 90 degrees at F_{nh}=1. Havelock [3] results for a single point disturbance are displayed on the same plot for the sake of comparison.

Fig. 16 shows transverse wave length and period variations up to F_{nh}=1.0 since this type of waves does not exist after the critical depth Froude number. For the constant speed of 1.184 m/s, the length and period are 0.90 m and 0.76 sec respectively in deep water. These values remain unchanged up to F_{nh} =0.7, after which they start to increase due to finite depth effects.

Fig. 17 shows the way the length and period of divergent waves vary with depth Froude number. These waves exist at both sub and supercritical regions. Maximum values for both length and period take place at depth Froude number of 1.0.

Divergent waves propagate at constant angle up to 0.6 F_{nh} after which it gets lower till reaching a minimum value at F_{nh}=1. In

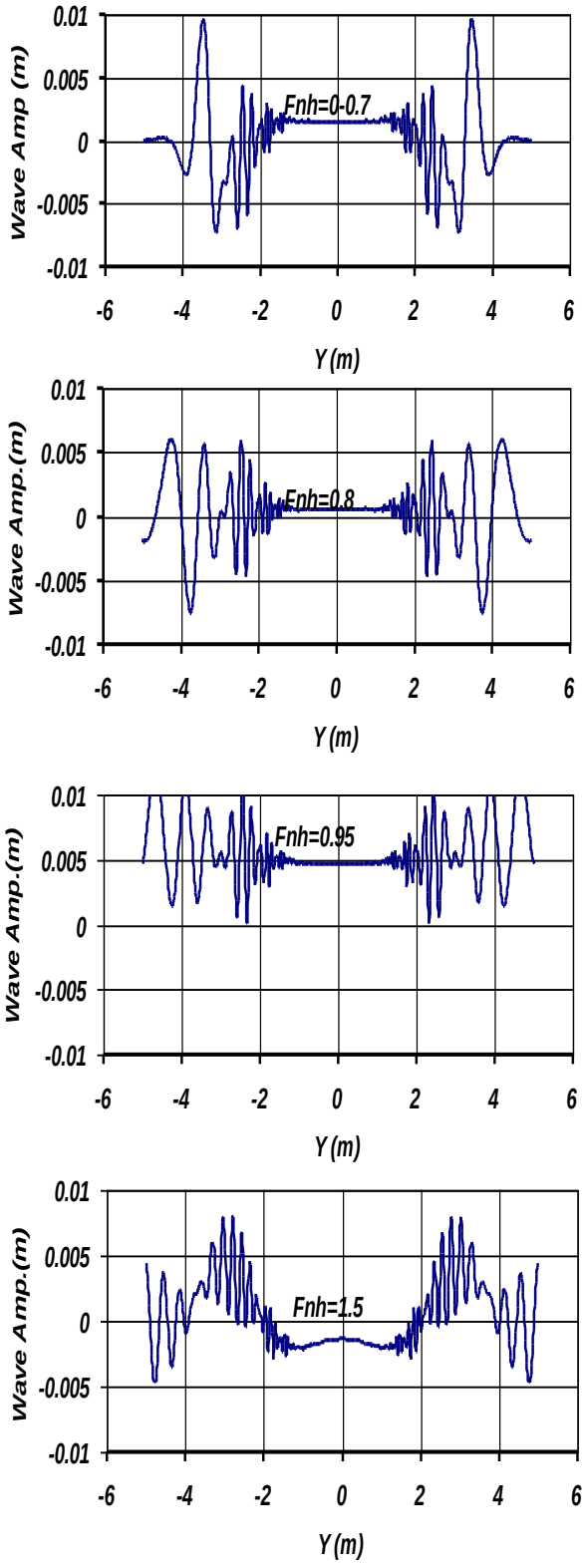

Fig. 13. Transverse wave cuts 2.5 m downstream (case study) at different Froude numbers at FnL = 0.35.

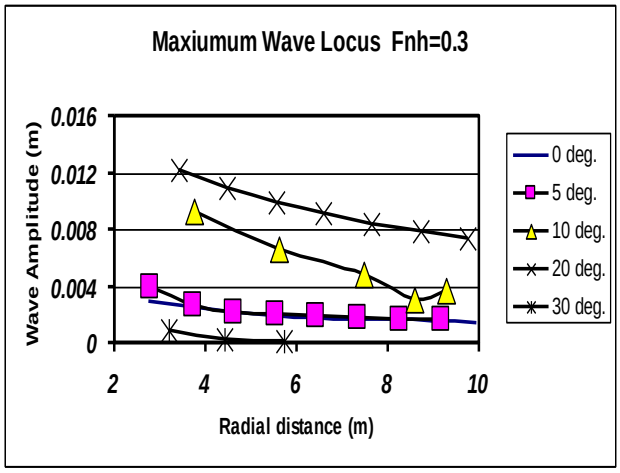

Fig. 14. Envelope of wave amplitude at different radial sections (case study) at FnL=0.35, Fnh=0.3.

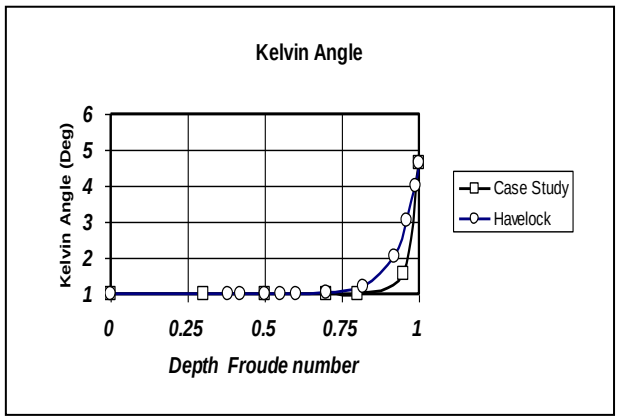

Fig. 15. Kelvin angle (case study) at different depth Froude number at FnL=0.35.

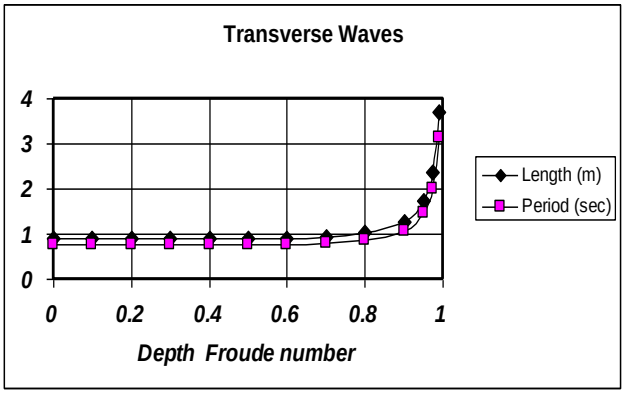

Fig. 16. Transverse wave length and period (case study) at different depth Froude numbers at FnL=0.35.

supercritical region, propagation angle trend is reversed and continuous increase is noticed. On the other side, the generated divergent wave crest line oblique angle to the sailing line is almost constant up to 0.7 F_{nh} with peak value at F_{nh}=1. Continuous decrease takes place for higher depth Froude numbers, Fig. 18.

Finally comparisons are made between the present case study results and the prediction results for an 85 m cruise ship and a fast patrol boat from [13] in figs. 19-20 and 21. The data are normalized by deep water values. The trend for the three cases is similar, however the differences in magnitude are attributed to form geometries.

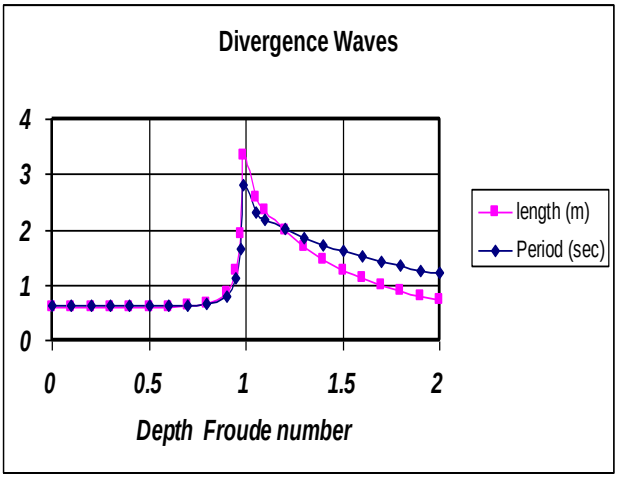

Fig. 17. Divergent wave length and period (case study) at different depth Froude numbers at FnL=0.35.

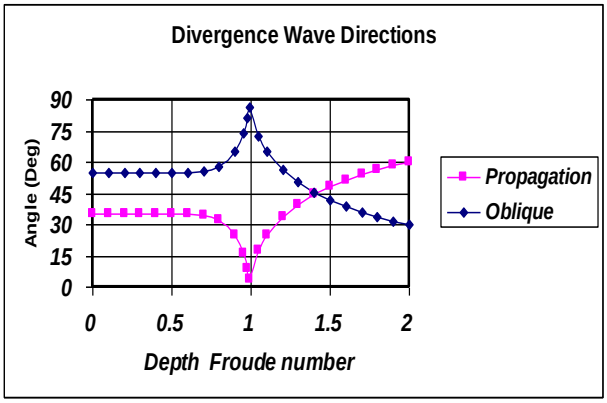

Fig. 18. Divergent Wave Propagation and Oblique Angle (Case Study) at different Depth Froude Numbers at FnL=0.35.

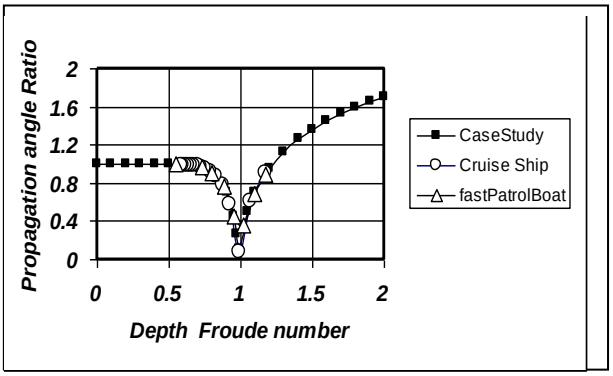

Fig. 19. Propagation angle ratio at different depth Froude number.

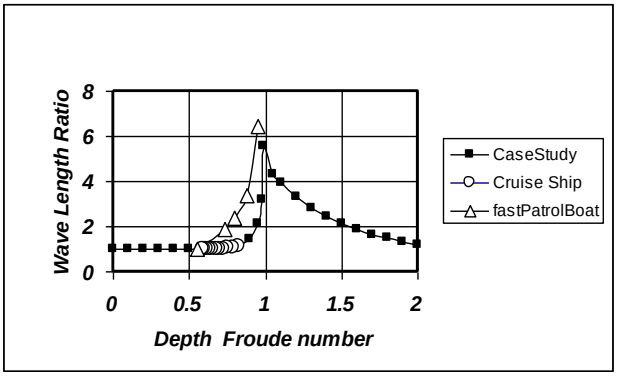

Fig. 20. Divergent wave period ratio at different depth Froude number.

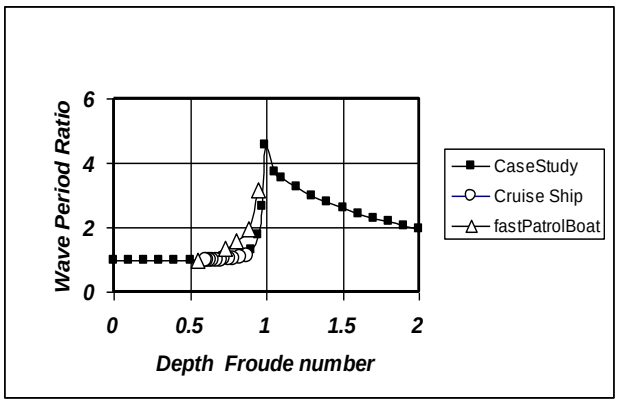

Fig. 21. Divergent wave period ratio at different depth Froude number.

7. Conclusions and remarks

In this work the major factors influencing wave wake characteristics are studied. Many of the problems associated with vessel generated waves occur in shallow and/or restricted water. It has been quantitatively shown for the case studied that the waves generated in shallow water are different than those generated in deep water.

Better understanding of ship generated waves as well as assessing theirquantifying parameters is quite important in avoiding undesirable environmental impacts

The simple 2D strut body studied here is intentionally selected to examine the ship generated waves aiming at establishing basis results excluding the effects of the complexity of hull forms. Effects of particular hull parts (bow, stern, appendages, etc) on the generated waves can be further investigated and compared to the basic results.

Analysis based on single pressure points is quite simple. Results obtained by 2D strut moving in water of different depths provide more realistic behavior of ship generated field beyond those given by simple single disturbance points. The calculations provided information on the characterizing parameters of the generated field as related to operating conditions.

Ship generated wave period is useful in assessing response of other moored vessel and jetties. Both wave length and direction can be used in estimating or predicting shore line and bank safety. Wave heights are used in setting a "no harm" effect criterion and speed limit.
Results showed that operating in the vicinity of the critical depth based Froude number results in amplification of wave length, period and wave spreading angles.

Finally, it is highly recommended to equip ships with gages that can directly display both length and depth Froude numbers similar to Mach meter in aircrafts This should help ship operators to avoid any shallow water related problems.

References

[1] J.W. Johnson, "Ship Waves in Navigation Channels", Proceedings of the 6th Conference on Coastal Engineering, Gainesville, FL. Council on Wave Research, Berkeley, CA, 666-90 (1958).

[2] J.R. Weggel and R.M. Sorensen, "Ship Wave Prediction for Port and Channel Design", Proceedings, Ports 86

Conference, American Society of Civil Engineers (1986).
[3] A. Kostykov, Theory of Ship Waves and Wave Resistance, E.C.I., Iowa City, Iowa (1968).
[4] C.S. YIH and S. ZHU, Patterns of Ship Waves, Quarterly of App. Maths., Vol. XLV11 (1), pp. 17-33 (1989).
[5] Lamb. Hydrodynamics. 5th Ed. Cambridge (1932).
[6] Stoker, Water Waves, Interscience Publishers, New York (1957).
[7] H.C. Raven, A Solution Method for the Nonlinear Ship Wave Resistance Problem, Doctoral Thesis, Technical University Delft (1996).
[8] E.O. Tuck, D.C. Scullen and L. Lazauskas, "Wave Patterns and Minimum Wave Resistance for High-Speed Vessels", 24th Symposium on Naval Hydrodynamics, Fukuoka, JAPAN (2002).
[9] E.O. Tuck, L. Lazauskas and D.C. Scullen, Sea Wave Pattern Evaluation, Part 1 Report: Primary Code and Test Results (Surface Vessels), Applied Mathematics Department the University of Adelaide (1999).
[10] E.O. Tuck, D.C. Scullen and L. Lazauskas, Sea Wave Pattern Evaluation, Part 4 Report: Extension to Multihulls and Finite Depth, Applied Mathematics Department, The University of Adelaide (2000).
[11] Michlet, User's Manual for Version 8.07, November (2005).
[12] Appendix A: Wake Wash Study for Calder Harbour Channel, DK52745-03 TVE-PT Joint Study/Doc13/tmf/10-04 DHI Water and Environment A-1.

Received May 13, 2007
Accepted June 6, 2007